



Cite this: *RSC Adv.*, 2024, **14**, 14161

## Single-fibre coating and additive manufacturing of multifunctional papers†

Joanna Judith Mikolei,<sup>a</sup> Christiane Helbrecht,<sup>b</sup> Janine Christin Pleitner,<sup>a</sup> Mathias Stanzel,<sup>a</sup> Raheleh Pardehkhoram,<sup>a</sup> Markus Biesalski,<sup>c</sup> Samuel Schabel<sup>b</sup> and Annette Andrieu-Brunsen  <sup>a\*</sup>

Paper-based materials with precisely designed wettabilities show great potential for fluid transport control, separation, and sensing. To tune the wettability of paper, paper sheets are usually modified after the paper manufacturing process. This limits the complexity of the local wettability design. We combined the wettability design of the individual fibres with subsequent paper sheet fabrication through either fibre deposition or fibre printing. Using silica-based cellulose fibre functionalization, the wettability of the paper sheets, containing only one specific fibre type, could be gradually tuned from highly hydrophilic to highly hydrophobic, resulting in water exclusion. The development of a silica-functionalized fibre library containing mesoporous or dense silica coatings, as well as silica with varying precursor compositions, further enabled the variation of the paper wettability and fluid flow. By combining this fibre library with the paper fabrication process by (i) fibre deposition or (ii) fibre printing, the paper wettability architecture and thus the local fibre composition were adjusted without any further processing steps. This enabled the fabrication of papers with wettability integration, such as a wettability pattern or a Janus paper design, containing wettability gradients along the paper sheet cross section. This asymmetric wettability along all three spatial dimensions enabled side-selective oil–water separation.

Received 14th March 2024  
 Accepted 23rd April 2024

DOI: 10.1039/d4ra01957a  
[rsc.li/rsc-advances](http://rsc.li/rsc-advances)

### Introduction

The use of paper-based materials as high-tech materials with well-defined transport, separation and sensing properties requires precise control of their wettability. In particular, the integration of asymmetric wetting properties, which is known as wettability integration, has attracted research interest.<sup>1,2</sup> This wettability integration can be attained with so-called micro/macropatterned surfaces, wettability boundaries or Janus interface materials with asymmetric wettability.<sup>1,2</sup> To date, the wettability of paper has been controlled mainly by changing the surface chemistry or the nanoscale surface texture. Changes in surface chemistry can be achieved by coating with hydrophobic polymers such as polystyrene,<sup>3</sup> using sustainable resources such as vegetable oils,<sup>4–6</sup> or by plasma etching.<sup>7</sup> Superhydrophobic

papers are obtained by tuning the fibre roughness. This is achieved by the deposition of inorganic particles,<sup>8</sup> which mainly consisted of nanoparticles, such as  $\text{SiO}_2$  (ref. 9–12) or waxes,<sup>13,14</sup> which form nanostructures after a thermal treatment. Commonly, coatings as well as inorganic particles or waxes are applied by dip,<sup>15</sup> spin,<sup>8</sup> spray,<sup>8</sup> roll-coating<sup>16</sup> or by simply soaking into<sup>17,18</sup> the coating solution. These techniques achieve complete covering of the paper surface with a coating or the nanoparticles; this results in paper sheets with a nearly uniform wettability and thus no wettability integration. To achieve wettability integration, locally controlled deposition of coatings, waxes, or particles in well-sized patterns or specific on one side of a paper sheet is needed. In 2009, Carrilho *et al.* showed that by printing a solid wax at the paper surface followed by infiltration of the melted wax into the paper cross section, complex hydrophobic patterns at the paper surface are created.<sup>19</sup> Moreover, wax printing is an often-used technique for creating hydrophobic barriers at paper surface.<sup>19–21</sup> Nevertheless, the resolution of wax patterns is limited due to melting and infiltration processes. Zhang *et al.* improved the hydrophobic barrier to a resolution of 600  $\mu\text{m}$  by inkjet printing silica nanoparticles.<sup>22</sup> Due to the deposition of small ink droplets containing silica nanoparticles *via* inkjet printing, papers with hydrophobic patterns were obtained. In addition to wax and inkjet printing, patterned paper surfaces with wettability integration can be obtained *via* lithography. Bretel *et al.* combined

<sup>a</sup>Ernst-Berl Institut für Technische und Makromolekulare Chemie, Macromolecular Chemistry – Smart Membranes, Technische Universität Darmstadt, Peter-Grünberg-Straße 8, D-64287 Darmstadt, Germany. E-mail: [annette.andrieu-brunsen@tu-darmstadt.de](mailto:annette.andrieu-brunsen@tu-darmstadt.de)

<sup>b</sup>Paper Technology and Mechanical Process Engineering, Technische Universität Darmstadt, Alexanderstraße 8, 64283 Darmstadt, Germany

<sup>c</sup>Ernst-Berl Institut für Technische und Makromolekulare Chemie, Macromolecular and Paper Chemistry, Technische Universität Darmstadt, Peter-Grünberg-Straße 8, D-64287 Darmstadt, Germany

† Electronic supplementary information (ESI) available. See DOI: <https://doi.org/10.1039/d4ra01957a>



lithography with UV-mediated thiol-X ligation, which resulted in hydrophobic patterns at the paper surface.<sup>23</sup> Additionally, hydrophobic patterns can be obtained by coating paper with a photocurable silane mixture and illuminating certain areas, as demonstrated by Nargang *et al.*<sup>24</sup> Zhang *et al.* presented a method where the paper was initially coated with an organosilane solution to generate hydrophobic paper with a contact angle larger than 150° and then a UV/ozone treatment was applied to the paper to create hydrophilic regions.<sup>18</sup> In addition to the generation of wettability patterns, Janus paper sheets can be obtained by side-selective functionalization. For example, Xu *et al.*<sup>25</sup> functionalized paper *via* a two-step approach, where a coating with hydrophobic SiO<sub>2</sub> nanoparticles was initially applied, and then a side-specific air plasma treatment was used on the paper; this process resulted in a hydrophobic paper side and a hydrophilic paper side.<sup>25</sup> In a one-step approach, Söz *et al.* obtained Janus interface paper with super hydrophobic wettability by applying thin crossed-linked poly(dimethylsiloxane) with inorganic particles *via* spray and spin coating on one paper side.<sup>26</sup> Nau *et al.* also created Janus interface paper with a silica-based coating *via* dip-coating by controlling the solvent evaporation of the coating solution during thermal posttreatment and thus the silica-coating distribution.<sup>15</sup> In all of these approaches, the papers are usually modified after manufacturing. This implies that the wettability integration is limited because the paper properties affect the achievable wettability pattern or gradient. The postprocessing step can be eliminated if the paper composition is modified directly during production by using prefunctionalized fibres in combination with a suitable paper fabrication process. On a laboratory scale, papers are usually produced using the Rapid-Koethen process. However, papers can also be produced by additive manufacturing technologies, as described, and patented (WO 2021/116293 A1) by Kreplin *et al.*<sup>27–29</sup> Here, the fibre suspension is applied to a wire *via* a nozzle and dewatered directly by vacuum. The nozzle traverses in predetermined paths in the x-y, building the paper from different paths and layers.<sup>27–29</sup> Although initial recent work involved additive manufacturing of paper sheets, new paper architectures, including asymmetric and patterned designs of paper functionalization such as paper wettability, have not yet been demonstrated. Defined and asymmetric paper sheet architecture design, among others, is of interest in the context of sensing or separation and would need to be based on a library of orthogonally functionalized fibres.<sup>2</sup>

Here, we present the first proof-of-concept study to demonstrate the design of paper architecture by controlling the fibre composition in all paper dimensions through the combination of individual fibre functionalization together with consecutive paper manufacturing. The paper sheet architecture and thus the integration of wettability gradients or patterns due to the controlled fibre composition are possible by (i) layerwise fibre deposition or (ii) cellulose fibre printing. Individual fibres are modified with dense or mesoporous silica coatings using sol-gel solutions containing the silica-forming precursors tetraethoxysilane (TEOS), methylmethoxysilane (MTMS) and dimethylmethoxysilane (DMDMS) with or without the mesopore-forming template Pluronic® F-127. By varying the

compositions of the sol-gel solutions with respect to the precursor ratios as well as the presence or absence of the mesopore template Pluronic® F-127, adjustments of the silica nanoscale porosity and the silica hydrophobicity from highly hydrophilic to hydrophobic can be achieved. The fibres are subsequently assembled into paper sheets with local control of the fibre composition and along the paper sheet cross section or the paper plane, resulting in the designed wettability architecture of each paper sheet. This approach provides new perspectives for fabricating paper with designed wetting integration, such as Janus interface materials with a wettability step gradient or wettability patterns in the paper plane, which both show specific water/oil separation and fluid transport properties.

## Results and discussion

### Single-fibre modification *via* stir-coating and paper manufacturing

Unmodified cotton linter papers are hydrophilic. Caused by the intrinsic hydrophilicity of the fibres, a water droplet imbibes into the unmodified paper sheet directly upon deposition at the paper sheet surface. To shape the wettability of the paper from hydrophilic to hydrophobic and to obtain defined wetting architectures such as gradients or patterns, the fibre needs to be initially modified, and then, the fibre composition must be controlled in all paper dimensions. Preliminary work has shown that hydrophobic paper sheets can be obtained with dense silica coatings generated by condensation of the silica-forming precursor TEOS and sol-gel chemistry, generating nonporous or dense silica functionalization.<sup>15,30–32</sup> This preliminary work demonstrates, that hydrophobization using dense silica functionalization goes along with prevention of fiber swelling and influences the water distribution in the fiber network which is reflected in contact angle changes. Upon functionalization of a paper sheet with a mesoporous silica coating, the paper remains hydrophilic.<sup>30,32</sup> Silica can be located outside and inside the cellulose fibre wall and in the lumen if present, as observed by confocal laser scanning microscopy (CLSM) studies.<sup>31</sup> The wettability, especially of these mesoporous silica-functionalized cellulose fibres, can be further tuned by the co-condensation of the nonpolar precursors MTMS and DMDMS in addition to TEOS and by varying their ratios.<sup>33</sup> Therefore, silica functionalization affects the water distribution and the fluid front location in the paper, as deduced from CLSM studies in our preliminary work.<sup>30</sup> This functionalization was transferred to cellulose fibres. To generate a fibre library for manufacturing papers with a defined wettability architecture, the individual fibres were functionalized by applying different mesoporous or dense silica-based coatings using the precursors TEOS, MTMS and DMDMS, sol-gel chemistry and stir coating. Sol-gel solutions with a high TEOS (TEOS : MTMS : DMDMS with a ratio of 0.8 : 0.12 : 0.08) as well as low TEOS (TEOS : MTMS : DMDMS in a ratio of 0.2 : 0.42 : 0.38) ratio with and without the micelle forming template Pluronic® F127 were used. For the silica coating, the cellulose fibres were stirred in their corresponding sol-gel solution at room temperature for 25



minutes (Fig. 1, upper part) before the fibres were either deposited (Fig. 1, left) or printed (Fig. 1, right) on a wire to form a paper with programmable, locally controlled wettability in the millimetre size range. For both paper manufacturing processes, the fibres were used immediately after the stir-coating process. After deposition or printing, the sol-gel solution was removed from the freshly formed paper by applying a vacuum. Thus, the top of the paper was not in contact with the metal wire, and the bottom of the paper was in contact with the metal wire during the paper manufacturing process. A subsequent thermal post-treatment at a final temperature of 130 °C was performed, and the temperature was held constant for 2 h. This process simultaneously led to the dehydration of the paper and hydrolysis and co-condensation of the silica precursors TEOS, MTMS, and DMDMS.

Due to the single-fibre modification *via* stir-coating followed by paper manufacturing using fibre deposition or printing, paper sheets with programmable wettabilities were produced without any further post-functionalization steps (Fig. 1).

Paper sheets with a homogenous fibre composition containing only one fibre type and being fabricated *via* fibre deposition could be tuned from being hydrophilic to hydrophobic depending on the fibre silica functionalization which controls the fiber swelling, as expected from the preliminary work (Fig. 2).<sup>15,30,32</sup> Small paper sheets were manufactured with

each kind of silica coating, and the resulting wettability was investigated by placing a 2 µL water droplet on the paper surface. Papers made of unmodified cotton linter fibres were hydrophilic (Fig. 2a). Additionally, paper sheets were manufactured from fibres with dense silica coatings containing both high and low amounts of nonpolar groups due to the co-condensation of TEOS, MTMS and DMDMS at two different ratios (TEOS : MTMS : DMDMS = 0.2 : 0.42 : 0.38 or 0.8 : 0.12 : 0.08). This resulted in hydrophobic paper sheets that excluded water (Fig. 2b and f). With a ratio of 0.2 : 0.42 : 0.38, a coating amount of 17 ± 3 wt% was obtained. Using a ratio of 0.8 : 0.12 : 0.08, a coating amount of 16 ± 3 wt% was obtained (Fig. 2b and f). Furthermore, papers obtained from fibres with a mesoporous silica coating containing a relatively high amount of nonpolar groups (TEOS : MTMS : DMDMS = 0.2 : 0.42 : 0.38) exhibited hydrophobicity and water exclusion (Fig. 2c). Upon reducing the nonpolar group content in the mesoporous silica coating (sol-gel solution with a higher TEOS ratio of TEOS : MTMS : DMDMS = 0.8 : 0.12 : 0.08) and thus decreasing the hydrophobicity of the mesoporous silica coating, a hydrophilic paper was obtained (Fig. 2g). The water droplet directly imbibed into the paper sheet with a mesoporous silica coating amount of 13 ± 1 wt%, as it did for unmodified cotton linter fibres. For paper sheets fabricated from mesoporous silica-coated fibres with varying unpolar MTMS and DMDMS ratios, the wettability

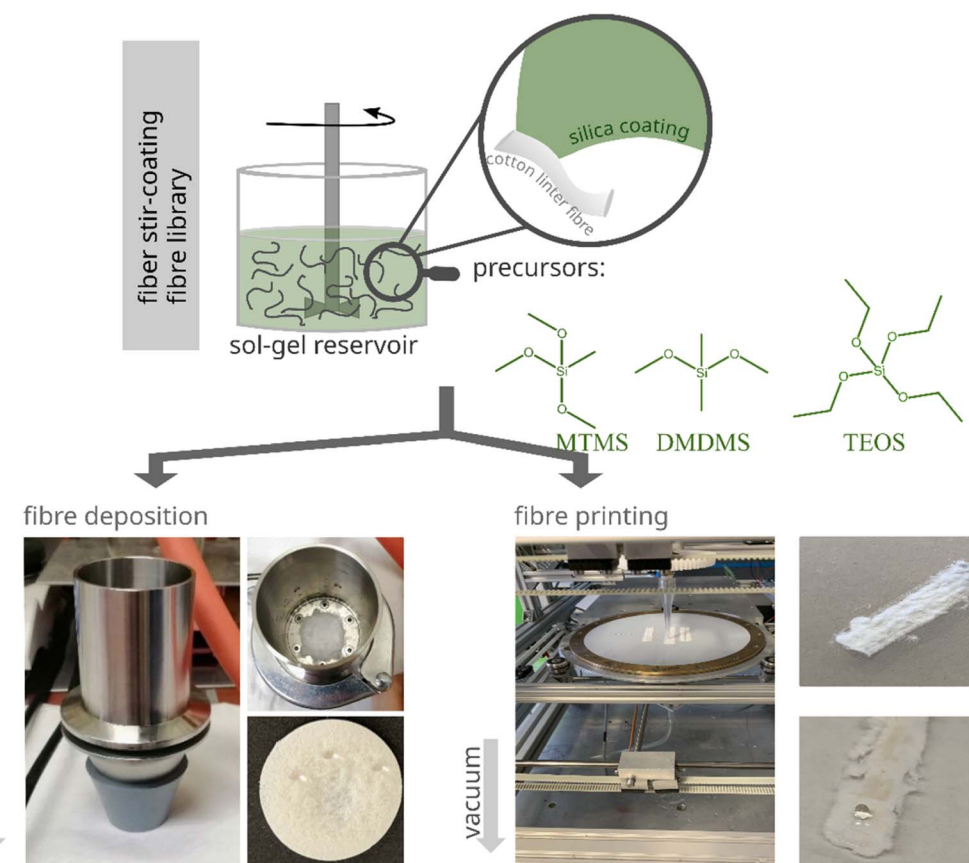


Fig. 1 Schematic illustration of single cotton linter fibre functionalization due to stir coating in different sol-gel solutions and two different paper manufacturing processes *via* fibre deposition or fibre printing.



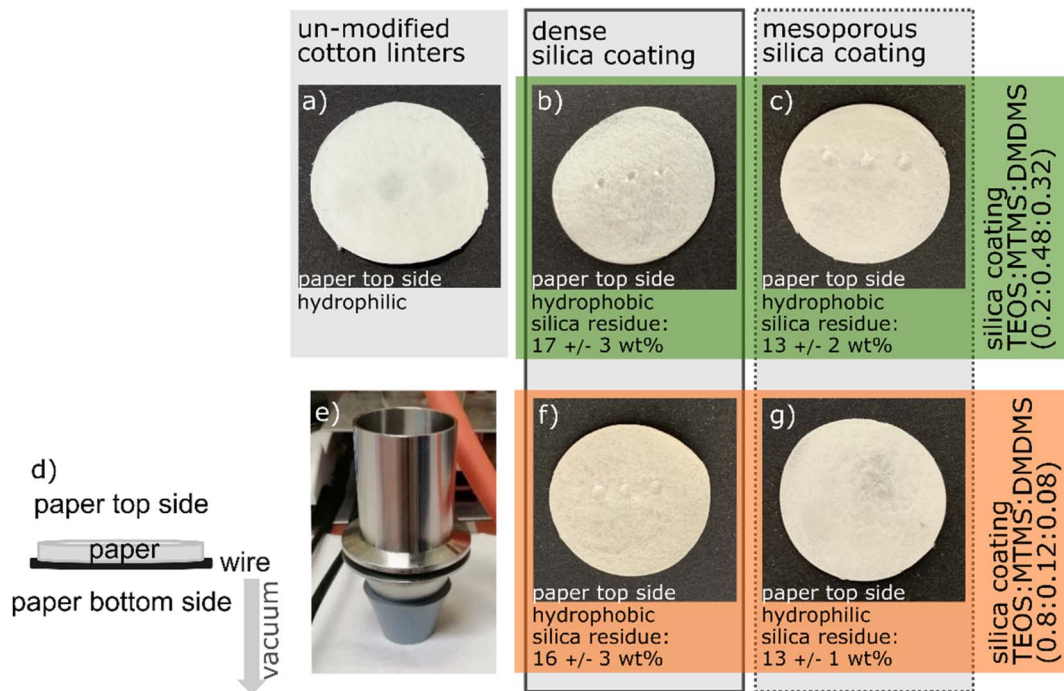


Fig. 2 Paper sheets fabricated using fibre deposition (d and e) and their modified wettability due to single-fibre modification tested by placing three  $2\text{ }\mu\text{L}$  water droplets on the paper top side (a–c, f and g). (a) Hydrophilic paper made of unmodified cotton linter fibres shown after droplet imbibition. (b) and (f) Papers made of functionalized cotton linter fibres coated with two different dense silica coatings, which differ in their sol-gel compositions. Both dense silica coatings result in hydrophobic characteristics with water exclusion properties. (c) and (g) Papers made of cotton linter fibres with mesoporous silica coatings containing different precursor ratios are shown. Due to the mesoporous silica coating and the different precursor ratios, one paper (f) has a hydrophobic character, while the other paper (g) remains hydrophilic.

varied with the MTMS and DMDMS content while keeping the silica coating amount constant at approximately  $13 \pm 2\text{ wt\%}$ . This clearly showed the influence of MTMS and DMDMS on paper wettability, which was comparable to the results from previous work on directly coating paper sheets.<sup>15,30–32</sup>

#### Fibre composition and architecture for designing asymmetric wettability and oil–water permeability

Based on the individual fibre functionalization together with the two different paper sheet manufacturing processes, paper sheets with adjustable fibre compositions and thus tuneable wetting architectures were obtained. Fibre deposition enabled the control of the wettability gradient along the paper sheet cross section (Fig. 3a); additionally, with fibre printing, the attainment of wettability patterns in the paper sheet plane was possible (Fig. 3d). Janus paper sheets with a wettability gradient along the paper cross section combining hydrophobic and hydrophilic fibres were obtained using layerwise fibre deposition (Fig. 3a–c). Paper sheets with wettability patterns in the paper plane were obtained by printing hydrophobic fibres next to hydrophilic fibres. A certain overlap ensured paper sheet stability (Fig. 3d–f). Both paper types with different integrated wettability architectures were obtained using hydrophilic unmodified cotton linter cellulose fibres. Additionally, hydrophobic, dense silica-coated fibres showed complete water exclusion. This resulted in an asymmetric wettability along the paper sheet cross section in this layered paper architecture (Fig. 3b and c) or in the paper plane in

case of printing wettability patterns (Fig. 3e and f). In the layered Janus-type paper sheets, water droplets with a volume of  $2\text{ }\mu\text{L}$  did not imbibe into the hydrophobic paper side which consists of dense silica coated fibres (Fig. 3b). A direct imbibition of the droplet occurs into the hydrophilic paper side (Fig. 3c). By analogy, water imbibed only into the hydrophilic area of paper sheets with a wettability pattern architecture in the paper plane (Fig. 3e). Consistently, water droplets did not infiltrate into the hydrophobic area of the wettability pattern, and the water fluid front stopped at the junction between the hydrophilic and hydrophobic areas of the two wettability patterns (Fig. 3e and f). The barrier between the hydrophilic and hydrophobic paper patterns became more distinct due to the interrupted horizontal water transport at the junction between the hydrophilic and hydrophobic patterns (Fig. 3f). This approach of generating a library of differently functionalized cellulose fibres and assembling them into paper sheets with designed layered or patterned architectures provides a novel route towards a variety of paper designs.

Interestingly, water imbibition is locally adjusted in the papers with integrated wettability. Unidirectional, liquid polarity-dependent fluid infiltration as well as fluid exclusion is achieved (Fig. 4 and 5). For example, this can be used for the separation of liquid mixtures. As an example, we demonstrate the liquid polarity-dependent infiltration as well as exclusion of oil and water for the two-layer paper sheet with a controlled fibre composition along its cross section due to layerwise deposition



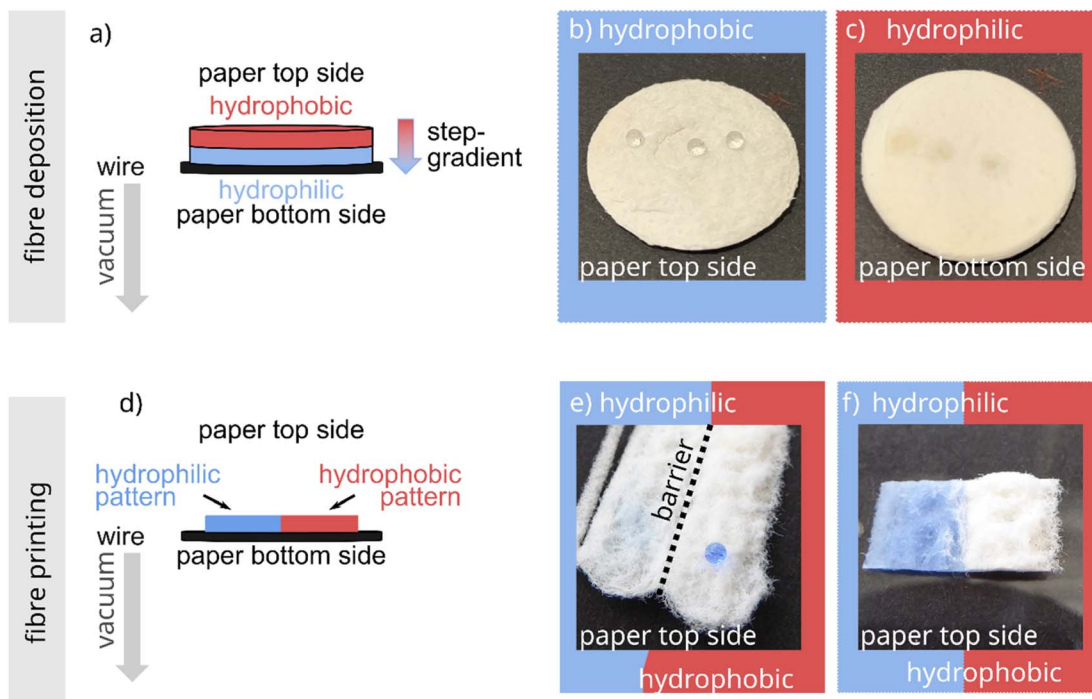


Fig. 3 (a) Schematic of the paper structure for Janus-like paper sheets with a controlled fibre composition along the paper cross section as a step gradient, resulting in hydrophobic (top side) and hydrophilic (bottom) paper sheets. (b) Hydrophobic paper on the top side of the Janus-like paper with its water exclusion properties. The three water droplets cannot imbibe into the paper top side, whereas the water droplets directly imbibe into the paper bottom side, as shown in (c). (d) Structure of papers with hydrophilic and hydrophobic patterns, which are obtained by controlling the fibre composition along the paper plane via the fibre printing technique. The paper top side with a hydrophilic and hydrophobic pattern is shown in (e). The water droplet imbibes into the hydrophilic paper pattern, whereas the droplet is excluded from entering the hydrophobic pattern. (f) Clearer image of the barrier properties. The water imbibition front stops at the barrier between the hydrophilic and hydrophobic patterns.

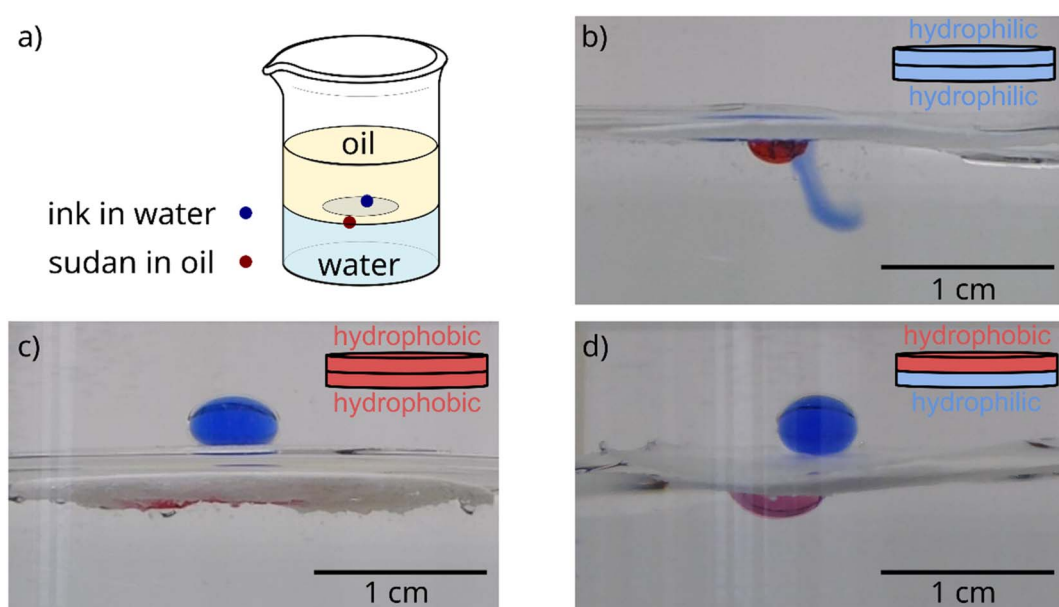


Fig. 4 (a) Experimental setup for analysing the oil/water infiltration or exclusion properties of papers made of functionalized fibres. The paper was placed between the water and oil phases with an oil (coloured with Sudan) and a water droplet (stained with blue ink). (b)–(d) Three different scenarios of exclusion and infiltration of the oil or water droplet. In scenario (b), both sides of the paper are hydrophilic. (c) Second scenario showing the oil/water infiltration or exclusion properties for a paper with two hydrophobic sides. (d) Third scenario in which the paper has Janus-type properties due to the hydrophilic and hydrophobic nature of the paper side.



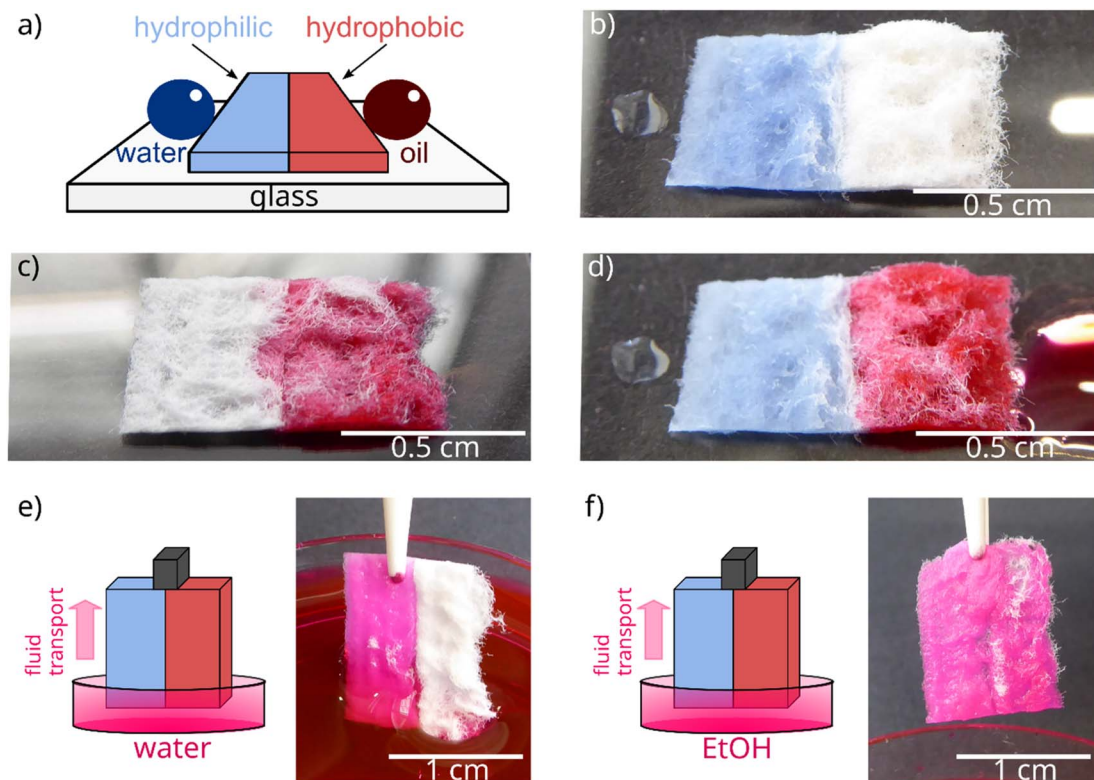


Fig. 5 (a) Experimental setup for analysing the oil/water transport of printed paper sheets consisting of hydrophilic and hydrophobic patterns. The patterned paper was placed on a glass substrate and brought into contact with water droplets (stained with blue ink) and oil droplets (coloured with Sudan VI) (b). Water can imbibe into the hydrophilic region, whereas oil is transported into the hydrophobic region (c). Both liquids stop at the junction between the hydrophilic and hydrophobic patterns; thus, no mixture of liquids occurs (d). (e) Vertical transport of water into the hydrophilic and hydrophobic paper pattern. Water enters the hydrophilic pattern and is transported in the vertical direction, which is not the case for the hydrophobic pattern. When placing the pattern paper in an ethanol reservoir, the less polar ethanol is transported in both patterns (f).

of unmodified and dense silica-coated fibres. A hydrophilic two-layer paper sheet without static contact angle differences was easily infiltrated and permeated by water. The fiber is accessible for the fluid and fiber swelling occurs. For the same hydrophilic two-layer paper sheet, the cyclohexane oil droplet remains at the paper surface, indicating the exclusion properties for nonpolar liquids (Fig. 4b). Two-layer paper sheets with two hydrophobic layers showed the opposite behaviour (Fig. 4c). The water droplet was not able to permeate the hydrophobic paper side, while the oil droplet easily infiltrated the hydrophobic paper sheet side (Fig. 4c). The dense silica coating prevents the fibre-fluid interaction and thus fibre swelling which leads to the water exclusion properties. The two-layer Janus paper sheet with a wettability step gradient combining a layer of hydrophobic dense silica-modified fibres and a layer of hydrophilic unmodified fibres stopped the water droplet from entering the hydrophobic side, but it was able to enter from the hydrophilic side. Moreover, the oil droplet was stopped from entering the hydrophilic side but was able to enter the hydrophobic side. Thus, the paper sheet with a Janus-type wettability step gradient shows direction-dependent and polarity-dependent infiltration and exclusion properties (Fig. 4d).

We performed water–oil permeation experiments comparable to those described above with papers consisting of a hydrophilic and hydrophobic pattern wetting architecture (Fig. 5a). By using

unmodified fibres for the hydrophilic pattern and dense silica-coated fibres for the hydrophobic pattern, static contact angle differences of  $130^\circ$  were obtained. As expected, the wettability pattern resulted in locally controlled imbibition of water and oil. A 1 mL water droplet imbibed into the hydrophilic areas, while it did not imbibe into the hydrophobic areas of the paper. Furthermore, water imbibition stopped at the transition between the hydrophilic and hydrophobic areas, even though the droplet volume was not fully adsorbed (Fig. 5b and d). Consistently, a Sudan V-stained oil droplet penetrated and was transported into the hydrophobic paper area but did not imbibe into the hydrophilic part of the paper (Fig. 5c and d, red). Due to the stopping of fluid transport, no mixing of the two fluids occurred (Fig. 5d). The different fluid transport properties, depending on the fluid polarity inside papers with hydrophilic and hydrophobic patterns, became even more evident when investigating the vertical fluid flow of water and ethanol (Fig. 5e and f). Water directly imbibed into the hydrophilic areas of the paper sheet, flowing in the vertical direction along the entire length of the hydrophilic area and was excluded from entering the hydrophobic area (Fig. 5e). As expected, a moderately polar liquid such as ethanol imbibes into both the hydrophilic and the hydrophobic areas and was vertically transported along the entire length of the patterned paper sheet (Fig. 5f).



## Conclusion

In this first proof-of-concept study, we showed for the first time locally functionalized paper fabrication by applying a fibre library together with a consecutive paper manufacturing process either by fibre deposition or fibre printing. An initial library of silica-functionalized cotton linter cellulose fibres with a designed silica composition and mesoporosity was generated. The fibre wettability was adjusted by varying the silica coating composition through co-condensation of different silica precursor ratios containing TEOS, MTMS and DMDMS as well as the presence or absence of a mesopore-forming template. The different types of silica-functionalized fibres were directly used for paper sheet manufacturing *via* either fibre deposition or fibre printing. Without any further processing, layerwise fibre deposition resulted in wettability step gradient formation. Fibre printing resulted in paper sheets with wettability pattern architectures. Thus, wettability integration was achieved along all three spatial dimensions of the paper sheet. By using both manufacturing techniques together with extending the fibre library, these complex architectures with adjustable fibre compositions and contact angle gradients were directly accessible. The design of the paper sheets with unidirectional water and oil permeation was demonstrated. For a wettability contrast of  $130^\circ$ , water or oil stopped at the barrier between the hydrophilic and hydrophobic parts of the paper sheet. In addition, pattern-selective and fluid polarity-dependent vertical transport was achieved by a patterned paper architecture. Further work will be related to optimizing the local resolution and extending the fibre library to exploit the design freedom with the additive manufacturing method, as shown for unmodified fibres.<sup>27–29</sup>

The presented approach provides a fascinating perspective of local fibre composition and layered or patterned paper sheet architecture design with specifically controlled wettability or porosity contrasts within one processing step and without using any organic polymer. Precise asymmetric paper sheet design was accomplished, which facilitates a new field of functional paper applications, including but not limited to sensing and separation.

## Experimental section

### Reagents

All chemicals and solvents were purchased from Merck and used as received.

### Cotton linter fibres

Cotton linter fibres, which were obtained from the Eifeltoer Mühle factory, were refined in a Voith LR 40 laboratory refiner (SEL 0.7 J m<sup>-1</sup>, set 3-1.6-60) with an effective specific refining energy of 100 kW h t<sup>-1</sup>. A fourfold fibre analysis was carried out with the FS5 Valmet. The refined cotton linter pulp had a fibre curl of  $14.9 \pm 0.2\%$ , an external fibrillation degree of  $1.8 \pm 0.1\%$ , a fines content of  $17.5 \pm 0.6\%$ , and a length-weighted average fibre length of  $0.95 \pm 0.01$  mm. The drainability was  $23 \pm 1^\circ$  SR.

### Dense and mesoporous sol-gel solutions

Dense and mesoporous silica coatings on single cotton linter fibres were obtained by using a sol-gel solution containing TEOS, MTMS and DMDMS as precursors with or without the mesopore-forming template Pluronic® F127. The solutions were prepared with the following molar ratios: 0.8/0.2 TEOS : 0.2/0.42 MTMS : 0.08/0.38 DMDMS : 40 EtOH : 0.0075 F127 : 10 H<sub>2</sub>O : 0.028 HCl. A dense silica coating was generated with the same composition but in the absence of the template Pluronic® F127. Before use, the freshly prepared sol-gel solution was stirred for 10 min at room temperature.

### Fibre modification

For the fibre modification, 2.2 g of the fibre suspension with a fibre content of 40 mg g<sup>-1</sup> fibre solution was stirred in 25 mL sol-gel solution for 25 min at room temperature. The stir-coated cotton linter fibres were directly used for the paper manufacturing process.

### Paper manufacturing *via* fibre deposition and printing

The fibre deposition process was applied to the sheet forming process following ISO 5269/2, DIN 54358, and Zellcheming Merkblatt V/8/75. In this process, the paper was formed by depositing fibres from a fibre solution on a metal wire applying vacuum. To downsize this process, a small paper sheet former was designed based on the Rapid Koethen sheet former (see Fig. S2† for more information about the setup). Two-layer papers were fabricated by a subsequent deposition of identical or different fiber layers. In the fibre printer,<sup>27–29</sup> a fibre suspension (with a stock consistency of 0.07%) was applied to a wire through an application nozzle. A wire frame used was similarly to the Rapid-Koethen sheet former, but instead of a metal wire, a PET wire with a mesh size of 102  $\mu$ m was used for better removability. A suction zone was located below the wire and directly dewatered the fibre suspension with the fibres remaining on the wire. The suction zone was vertically aligned with the application nozzle and moved synchronously. The nozzle with an outlet diameter of 1.298 mm moved along a predefined path, building up the paper from single paths and, in this case, in only one layer. The intended sample size was 40  $\times$  26 mm, with the paths parallel to the long side. The paths overlapped by 25%, which meant that the sample consisted of 16 planned paths. The nozzle speed was 1000 m min<sup>-1</sup>. First, 25 mL of the modified fibre suspension was applied, resulting in approximately four paths. Then, 25 mL of the unmodified fibre suspension was applied directly next to it. The superfluous sol-gel solution was removed in both paper manufacturing processes by applying a vacuum. The freshly formed papers underwent thermal posttreatment where 60 °C was applied for 1 h, then the temperature was further increased to 130 °C in 10 min, and the temperature remained at 130 °C for 2 h. After this process, the samples were cooled to room temperature.



### Thermogravimetric analysis (TGA)

Thermogravimetric measurements were performed using a TGA 1 instrument from Mettler Toledo. The silica-coated papers were placed in a 100  $\mu\text{L}$  Al crucible, and the following temperature program was used for the controlled combustion of the organic part. The hybrid material was heated from 25  $^{\circ}\text{C}$  to 600  $^{\circ}\text{C}$  at a rate of 10  $^{\circ}\text{C min}^{-1}$  under a constant air flow of 30  $\text{mL min}^{-1}$ . A maximum temperature of 600  $^{\circ}\text{C}$  was maintained for 10 min. For the data evaluation, the corresponding program Star1 was used.

### Paper wettability

The wettability of the papers was tested by placing 2  $\mu\text{L}$  water droplets on the top of the paper using an Eppendorf pipette.

### Oil/water infiltration and exclusion

A cylindric beaker contained a water phase covered by a cyclohexane phase. The non-prewetted cotton linter paper with or without asymmetric surface modification was placed between the two phases. With an injection needle, a cyclohexane droplet stained with Sudan V was placed at the cotton linter paper surface facing the water phase. A water droplet stained with blue ink was placed on the surface of the cotton linter paper facing the cyclohexane phase.<sup>34</sup> The experiment was recorded using a Panasonic DMC-TZ71 with a DC VARIO-ELMAR 1 : 3.3-6.4/4.3-129 ASPH LEICA objective.

### Oil/water transport and exclusion

A non-prewetted paper sheet with a hydrophobic and hydrophilic pattern was placed on a thin glass substrate. With an Eppendorf pipette, a 1 mL droplet of water stained with ink or cyclohexane stained with Sudan V was placed next to the paper such that the droplet was in constant contact with the paper. The experiment was recorded using a Panasonic DMC-TZ71 with a DC VARIO-ELMAR 1 : 3.3-6.4/4.3-129 ASPH LEICA objective.

### Water/EtOH vertical transport

The vertical transport of water or ethanol in paper with a hydrophilic and hydrophobic pattern was investigated by placing the paper stripe into either a water reservoir or an ethanol reservoir. The fluid transport was recorded using a Panasonic DMC-TZ71 with a DC VARIO-ELMAR 1 : 3.3-6.4/4.3-129 ASPH LEICA objective.

### Conflicts of interest

There are no conflicts to declare.

### Acknowledgements

The authors kindly acknowledge the financial support of the German Research Foundation (DFG) for projects AN1301/8 and 405469627. In addition, the authors would like to thank Peter Hanauer and Martin Schwarz (Workshop Manager, Chemical

Department, TU Darmstadt) for helping with the constructional design of the miniaturized paper sheet former setup as well as processing. We also thank Prof. E. Dörsam and Carl Fridolin Weber (IDD, Department of Mechanical Engineering, TU Darmstadt) for their support with the determination of the paper surface roughness.

### References

- 1 P. -G. de Gennes, *Soft Matter, Angew. Chem.*, 1992, **31**, 842.
- 2 Ç. K. Söz, S. Trosien and M. Biesalski, *Janus Interface Materials: A Critical Review and Comparative Study, ACS Mater. Lett.*, 2020, **2**, 336.
- 3 J. L. Benedé, A. Chisvert, R. Lucena and S. Cárdenas, A paper-based polystyrene/nylon Janus platform for the microextraction of UV filters in water samples as proof-of-concept, *Microchim. Acta*, 2021, **188**, 391.
- 4 V. K. Rastogi and P. Samyn, Bio-based coatings for paper applications, *Coatings*, 2015, **5**, 887.
- 5 A. Loesch-Zhang, C. Cordt, A. Geissler and M. Biesalski, A Solvent-Free Approach to Crosslinked Hydrophobic Polymeric Coatings on Paper Using Vegetable Oil, *Polymers*, 2022, **14**, 1773.
- 6 S. Thakur, M. Misra and A. K. Mohanty, Sustainable Hydrophobic and Moisture-Resistant Coating Derived from Downstream Corn Oil, *ACS Sustain. Chem. Eng.*, 2019, **7**, 8766.
- 7 P. Dimitrakellis, A. Travlos, V. P. Psycharis and E. Gogolides, Superhydrophobic Paper by Facile and Fast Atmospheric Pressure Plasma Etching, *Plasma Processes Polym.*, 2017, **14**, 1600069.
- 8 Ç. K. Söz, Z. Özomay, S. Unal, M. Uzun and S. Sönmez, Development of a nonwetting coating for packaging substrate surfaces using a novel and easy to implement method, *Nord. Pulp Pap. Res. J.*, 2021, **36**, 331.
- 9 G. Chen, Durable superhydrophobic paper enabled by surface sizing of starch-based composite films, *Appl. Surf. Sci.*, 2017, **409**, 45.
- 10 S. Jiang, S. Zhou, B. Du and R. Luo, Preparation of superhydrophobic paper with double-size silica particles modified by amino and epoxy groups, *AIP Adv.*, 2021, **11**, 025127.
- 11 H. Ogihara, J. Xie, J. Okagaki and T. Saji, Simple method for preparing superhydrophobic paper: spray-deposited hydrophobic silica nanoparticle coatings exhibit high water-repellency and transparency, *Langmuir*, 2012, **28**, 4605.
- 12 Q. Wang, J. Hiong, G. Chen, O. Xinpeng, Z. Yu, Q. Chen and M. Yu, Facile approach to develop hierarchical roughness fiber@SiO<sub>2</sub> blocks for superhydrophobic paper, *Materials*, 2019, **12**, 1393.
- 13 C. Cordt, A. Geissler and M. Biesalski, Regenerative Superhydrophobic Paper Coatings by In Situ Formation of Waxy Nanostructures, *Adv. Mater. Interfaces*, 2021, **8**, 2001265.
- 14 W. Zhang, P. Lu, L. Qian and H. Xiao, Fabrication of superhydrophobic paper surface via wax mixture coating, *Chem. Eng. J.*, 2014, **250**, 431.



15 M. Nau, N. Herzog, J. Schmidt, T. Meckel, A. Andrieu-Brunsen and M. Biesalski, Janus-Type Hybrid Paper Membranes, *Adv. Mater. Interfaces*, 2019, **6**, 1900892.

16 Y. Teng, Facile fabrication of superhydrophobic paper with durability, chemical stability and self-cleaning by roll coating with modified nano-TiO<sub>2</sub>, *Appl. Nanosci.*, 2020, **10**, 4063.

17 S. Wang, M. Li and Q. Lu, Filter paper with selective absorption and separation of liquids that differ in surface tension, *ACS Appl. Mater. Interfaces*, 2010, **2**, 677.

18 L. Zhang, H. Kwok, X. Li and H. Z. Yu, Superhydrophobic Substrates from Off-the-Shelf Laboratory Filter Paper: Simplified Preparation, Patterning, and Assay Application, *ACS Appl. Mater. Interfaces*, 2017, **9**, 39728.

19 E. Carrilho, A. W. Martinez and G. M. Whitesides, Understanding wax printing: a simple micropatterning process for paper-based microfluidics, *Anal. Chem.*, 2009, **81**, 7091.

20 A. W. Martinez, S. T. Phillips, M. J. Butte and G. M. Whitesides, Patterned Paper as a Platform for Inexpensive, Low-Volume, Portable Bioassays, *Angew. Chem.*, 2007, **119**, 1340.

21 C. Li, M. Boban, S. A. Snyder, S. P. R. Kobaku, G. Kwon, G. Mehta and A. Tuteja, Paper-Based Surfaces with Extreme Wettabilities for Novel, Open-Channel Microfluidic Devices, *Adv. Funct. Mater.*, 2016, **26**, 6121.

22 Y. Zhang, T. Ren and J. He, Inkjet Printing Enabled Controllable Paper Superhydrophobization and Its Applications, *ACS Appl. Mater. Interfaces*, 2018, **10**, 11343.

23 G. Bretel, J. Rull-Barrull, M. C. Nongbe, J.-P. Terrier, E. Le Grogne and F.-X. Felpin, Hydrophobic Covalent Patterns on Cellulose Paper through Photothiol-X Ligations, *ACS Omega*, 2018, **3**, 9155.

24 T. M. Nargang, R. Dierkes, J. Bruchmann, N. Keller, K. Sachsenheimer, C. Lee-Thedieck, F. Kotz, D. Helmer and B. E. Rapp, Photolithographic structuring of soft, extremely foldable and autoclavable hydrophobic barriers in paper, *Anal. Methods*, 2018, **10**, 4028.

25 B. Xu and Y. Ding, Hydrophilic/Hydrophobic SiO<sub>2</sub> Nanoparticles Enabled Janus-Type Paper through Commercial Glaco Spraying and Air-Plasma Treatment, *Adv. Mater. Interfaces*, 2022, **9**, 2200934.

26 Ç. Koşak Söz, S. Trosien and M. Biesalski, Superhydrophobic Hybrid Paper Sheets with Janus-Type Wettability, *ACS Appl. Mater. Interfaces*, 2018, **10**, 37478.

27 F. Kreplin and S. Schabel, *Tailoring Paper Structures by Fiber Printing*, 2021.

28 F. Kreplin and S. Schabel, Fiber Printing: new possibilities for fibre-based materials and devices by additive manufacturing, *13th European Congress of Chemical Engineering*, 2021.

29 F. Kreplin and S. Schabel, *Fiber Printer: A Machine to Apply 3D Printing Principles on Paper Production, Progress in Paper Physics Seminar*, 2020, p. 245.

30 J. J. Mikolei, L. Neuenfeld, S. Paech, M. Langhans, M. Biesalski, T. Meckel and A. Andrieu-Brunsen, Mechanistic Understanding and Three-Dimensional Tuning of Fluid Imbibition in Silica-Coated Cotton Linter Paper Sheets, *Adv. Mater. Interfaces*, 2022, **9**, 2200064.

31 J. J. Mikolei, D. Richter, R. Pardehkhoram, C. Helbrecht, S. Schabel, T. Meckel, M. Biesalski, M. Ceolin and A. Andrieu-Brunsen, Nanoscale pores introduced into paper via mesoporous silica coatings using sol-gel chemistry, *Nanoscale*, 2023, **15**, 9094.

32 C. Dubois, N. Herzog, C. Rüttinger, A. Geißler, E. Grange, U. Kunz, H. J. Kleebe, M. Biesalski, T. Meckel, T. Gutmann, M. Gallei and A. Andrieu-Brunsen, Fluid Flow Programming in Paper-Derived Silica-Polymer Hybrids, *Langmuir*, 2017, **33**, 332.

33 J. J. Mikolei, M. Stanzel, R. Pardehkhoram, R. Lehn, M. Ceolin and A. Andrieu-Brunsen, Fluid Flow Control in Cotton Threads with Mesoporous Silica Coatings, *Adv. Mater. Interfaces*, 2023, **10**, 2300211.

34 C. Chen, D. Weng, A. Mahmood, S. Chen and J. Wang, Separation Mechanism and Construction of Surfaces with Special Wettability for Oil/Water Separation, *ACS Appl. Mater. Interfaces*, 2019, **11**, 11006.

